

If Not Here, There. Explaining Machine Learning Models for Fault Localization in Optical Networks

Oleg Karandin^{1*}, Omran Ayoub², Francesco Musumeci¹, Yusuke Hirota³, Yoshinari Awaji³, Massimo Tornatore¹

¹*Department of Electronics, Information and Bioengineering, Politecnico di Milano, Milan, Italy*

²*University of Applied Sciences of Southern Switzerland, Switzerland*

³*National Institute of Information and Communications Technology, Tokyo, Japan*

*Corresponding author: oleg.karandin@polimi.it

Abstract—Machine Learning (ML) is being widely investigated to automate safety-critical tasks in optical-network management. However, in some cases, decisions taken by ML models are hard to interpret, motivate and trust, and this lack of explainability complicates ML adoption in network management. The rising field of Explainable Artificial Intelligence (XAI) tries to uncover the reasoning behind the decision-making of complex ML models, offering end-users a stronger sense of trust towards ML-automated decisions. In this paper we showcase an application of XAI, focusing on fault localization, and analyze the reasoning of the ML model, trained on real Optical Signal-to-Noise Ratio measurements, in two scenarios. In the first scenario we use measurements from a single monitor at the receiver, while in the second we also use measurements from multiple monitors along the path. With XAI, we show that additional monitors allow network operators to better understand model's behavior, making ML model more trustable and, hence, more practically adoptable.

Index Terms—Optical networks, network management, fault localization, ML, XAI, SHAP

I. INTRODUCTION

Automated fault management is a key objective for operators willing to improve network reliability and reduce operational expenses. Hence, Machine Learning (ML), in recent years, has been intensively investigated to automate fault-management tasks, as failure detection, identification and localization in optical networks [1]–[4], by observing behavioral patterns of Quality of Transmission metrics, as the Signal-to-Noise Ratio (SNR).

However, accuracy of complex ML models cannot be proven theoretically, but only evaluated experimentally on a selected dataset, and the reasoning behind the decisions of these models cannot be overseen by human experts. Thus, it is very hard to control whether decision-making of the ML model is flawed and/or influenced by the specific dataset used, and the decisions are perceived as coming from “black boxes” with scarce explainability. As network operators are unwilling to trust decisions carried out by “black boxes” [5], [6], novel approaches are being investigated to make ML-based decisions explainable and be sure that correct decisions are taken based on correct logic.

Explainable AI (XAI) refers to a set of techniques that allow to uncover the reasoning of a ML model to a human expert in an easy-to-understand format, e.g., by visualizing learned data dependencies, hence making ML models more trustable and more likely to be adopted practically.

In this paper, we apply XAI to investigate the reasoning of ML models in the failure localization problem. Multiple ML models solving several fault-management problems in optical networks exist, but, to the best of our knowledge, the underlying reasoning of those models has not been investigated using XAI. In particular, we use SHAP [7] (a well known XAI framework) to find correlations between the input data and model decisions and compare explanations in two scenarios with different amount of telemetry: 1) Optical SNR (OSNR) measurements from a single monitor at the receiver and 2) OSNR measurements from multiple monitors along the lightpath. We show that additional telemetry along the lightpath can improve model explainability, increasing trust in its predictions.

II. PROBLEM STATEMENT AND DATA

We model the failure-localization problem as a supervised multi-class classification problem. We use real telemetry data obtained on a testbed of the National Institute of Information and Communications Technology (NICT) in Sendai, Japan (see Fig. 1). ROADM^s, identified as Node A, B, C and D are equipped with an optical amplifier (OA) at their input and output ports. Links between ROADM^s are emulated by attenuators with loss equivalent to 80 km long optical fiber. We consider a single lightpath traversing all 3 links and carrying an OOK modulated 10G signal. A fault (11 dB additional attenuation) can occur at any one of the three links, and our objective is to determine the faulty link.

OSNR is measured every second by monitors at the input ports of three traversed nodes (B, C and D). To make our ML-based classifier independent from the specific OSNR values, that may vary according to system settings (e.g., OA gain, span length, central frequency, etc.), we normalize OSNR sequences from every monitor to zero mean and unit standard deviation. Classification is performed for OSNR windows of W seconds. For each window we consider the following

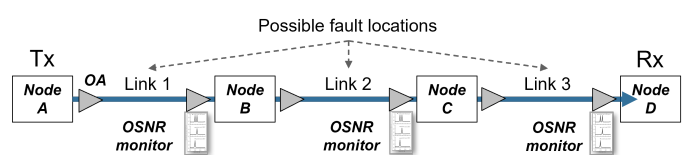


Fig. 1. NICT's Sendai testbed setup

5 features: average (av), standard deviation (std), minimum (min), maximum (max) and peak-to-peak (p2p) OSNR values.

We consider two scenarios: 1) single monitor (SM), where we use OSNR telemetry only from the receiver node D, and, hence, ML model makes a prediction based on 5 input features, and 2) multiple monitors (MM), where we use OSNR telemetry from all three traversed nodes B, C, D, with a total of 15 features (5 features from each monitor) as input to the ML model. Second scenario represents the highly automated approach to network management characterized by having many sources of telemetry across the network, as in Ref. [4].

In both scenarios, we train XGBoost (XGB) classifier based on a gradient boosting model, optimizing hyperparameters for different window sizes and fixing a window size of 100 samples (seconds), as it guarantees localization accuracy close to 1 in both SM and MM scenarios. For each fault we consider 10000 windows from each monitor during training and testing, and to obtain global explanations. We apply SHAP to explain model predictions towards each of the three classes (three faulty links) to understand how the features from different monitors drive the decisions of the localization model.

III. EXPLAINING MODEL BEHAVIOR FOR AUTOMATED FAULT LOCALIZATION

XAI techniques can provide explanations to justify why and how the model arrived to a certain decision. These explanations can be either local, i.e., they explain a decision for a specific data instance, or global, i.e., they explain model's decisions towards a particular class. In our work, we are interested in explaining model's decisions towards each class (i.e., the different fault locations), in other words, global explanations. To this end, we apply the *SHAP framework*, that is based on Shapley value, a concept from game theory that quantifies contributions of different players to the total payoff [7]. In the context of explainability, Shapley values are computed by perturbing input features and by monitoring how they influence model predictions, while iterating through all permutations of the input feature vector. A Shapley value is computed for each feature towards each of the classes for each explained data sample. While XGB models can only rank input features by their importance, SHAP provides an understanding of how specific values of input features drive the ML model towards particular decisions, by correlating feature importance (Shapley value) with feature original value and model's predictions.

In the following, we discuss model explanations relative to the MM and the SM scenarios.

A. Multiple Monitors

Figure 2(a), (b) and (c) show the *summary plots* produced by SHAP in the MM scenario to explain the decision of localizing a fault on link $L = 1$, $L = 2$ and $L = 3$, respectively.

The *summary plot* combines feature importance with feature values to explain model's behavior. Horizontal axis represents the Shapley value scale. Each point of the summary plot is a Shapley value for a given feature in a given data sample.

The vertical axis represents features ranked according to their importance. Features that play highest role in localizing a particular faulty link L have many points with high absolute Shapley values and are placed at the top of the list. Summary plots in Fig. 2 visualize correlations between values of a feature and the impact on the prediction towards each class. Red (or blue) dots mean that high (or low) values of some feature F contribute towards predicting that fault is at link L (positive Shapley values) or not at link L (negative Shapley values). In the figure, prefixes B, C and D define the location of the monitor (see Fig. 1).

Looking at Fig. 2(a), we can observe that $B_{p2p} \text{ OSNR}$ and $B_{std} \text{ OSNR}$ are the two most significant features to locate fault at link 1, as there are many data points with high absolute Shapley values for those features. As intuition would suggest, the most impacting features are related to OSNR measured by the monitor located at the end of the faulty link. In particular, explanations towards predicting that fault location is at link 1 are based on strictly polarized values of the features: low for $B_{p2p} \text{ OSNR}$ and high for $B_{std} \text{ OSNR}$, making it easy for a domain expert to verify.

Similar observation can be drawn looking at Fig. 2(c); in this case the most important features used to localize fault at link 3 are $D_{av} \text{ OSNR}$, $D_{min} \text{ OSNR}$, $C_{av} \text{ OSNR}$ and $D_{max} \text{ OSNR}$. Three of these features are again related to OSNR measured by the monitor at the end of the faulty link. In particular, we see that the model correlated medium values of $D_{av} \text{ OSNR}$, high values of $D_{min} \text{ OSNR}$ and medium values of $D_{max} \text{ OSNR}$ with a failure at link 3. On the contrary, $C_{av} \text{ OSNR}$ is based on OSNR measured before the fault, and is used by the ML model to build a proof by contradiction, as high value of this feature contributes towards locating a fault at link 3, while low value of this feature contributes towards locating a fault at other 2 links (check Fig. 2(a) and (b)).

More insightful (and less intuitive) observations arise by looking at the summary plot in Fig. 2(b). Here, the most important features to localize fault at link 2 are $B_{p2p} \text{ OSNR}$ and $D_{av} \text{ OSNR}$. This is an important insight in the reasoning of the model: to classify failure at link 2, the model relies mostly on measurements from monitors deployed at the previous and next link from the fault. In fact, the values of these two features distinguish this fault location from the other two: a high value of $B_{p2p} \text{ OSNR}$ contributes towards locating a fault at link 2, while low value at Fig. 2(a) contributes towards locating a fault at link 1; similarly a high value of $D_{av} \text{ OSNR}$ contributes towards locating a fault at link 2, while medium value at Fig. 2(c) contributes towards locating a fault at link 3. Finally, we note that only the third most important feature is related to the next monitor after the fault. If $C_{min} \text{ OSNR}$ is high, it contributes to failure at link 2, while if low or medium, it suggests otherwise.

Summarizing, the ML algorithm reasons in two different ways to localize the faulty link. For two fault locations it makes a decision using clearly polarized (strictly high or low) statistics of OSNR measured at the same link, after the fault. Such reasoning should be easily confirmed or questioned by

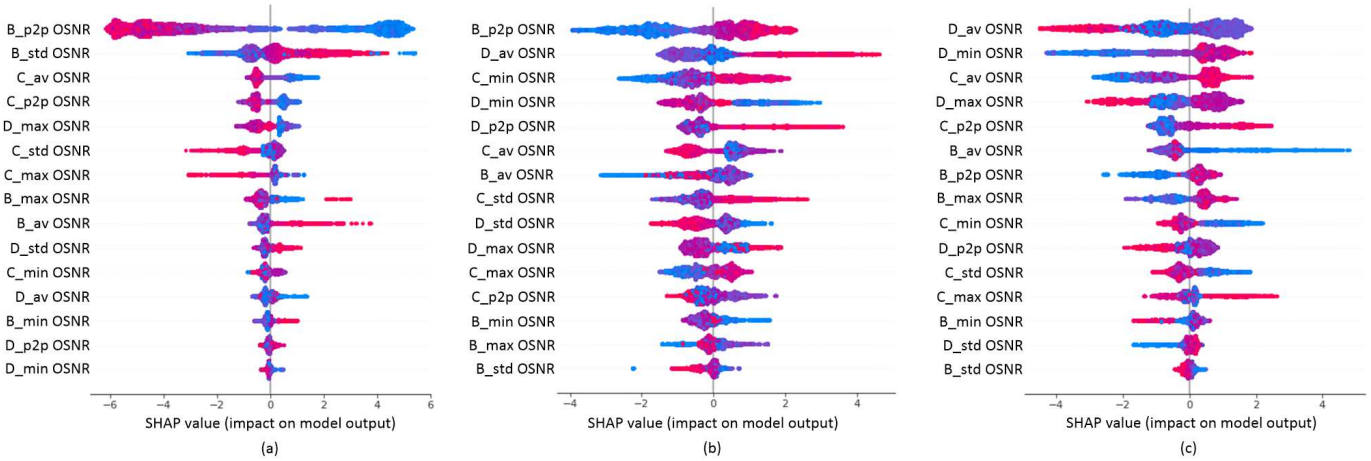


Fig. 2. SHAP summary plots for Multiple Monitors scenario and fault at (a) link 1, (b) link 2, (c) link 3

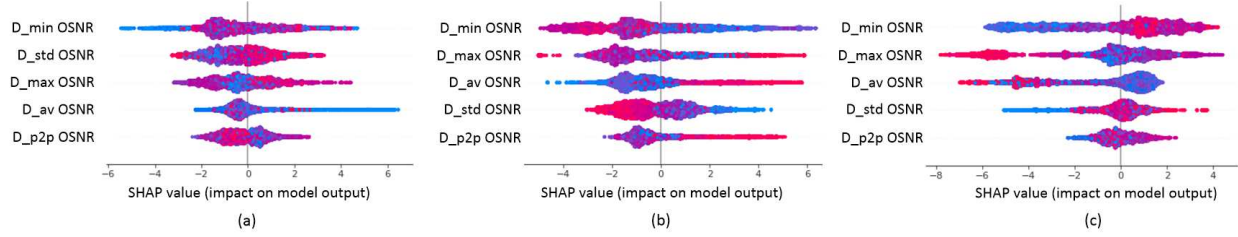


Fig. 3. SHAP summary plot for Single Monitor scenario and fault at (a) link 1, (b) link 2, (c) link 3

a domain expert. And sometimes ML algorithm uses proof by contradiction, looking for most distinctive differences in OSNR behaviour with respect to other cases. Reasoning of this second type is also easy to verify.

B. Single Monitor

Figures 3(a), (b) and (c) show the *summary plot* produced by SHAP in the SM scenario for the fault on link $L = 1$, $L = 2$ and $L = 3$, respectively. In this case, we have only one monitor and, hence, only 5 features. The summary plots show that all features have similar absolute Shapley values, and hence approximately equivalent importance.

Faults at links 2 and 3 (Fig. 3(b) and Fig. 3(c)) are distinguished by the value of D_{min} OSNR; it is, respectively, low and high. However, for the fault at link 1, no single feature at Fig. 3(a) is strictly positive or negative based on its value. In fact, we see blue and red dots distributed similarly for positive and negative Shapley values, meaning that classifier relies on more complex interactions among different features. Even in a small network with 3 fiber spans it is hard to verify if the reasoning used to localize fault at link 1 is reasonable and general, or overtuned to the training dataset.

IV. CONCLUSION

We have shown that a ML model, trained to solve fault localization using multi-monitor OSNR telemetry, reasons using features that have strictly low or high value depending on the fault location, and its decisions can be clearly explained. On the other hand, ML model that considers telemetry at a single monitor at the receiver also successfully distinguishes faults at different links, but by learning complex interactions of OSNR statistics, making its reasoning hard to explain even

in our simple network setup. Deploying monitors in every node, as considered in our multi-monitor results, is probably too costly for a large network, but this study suggests that deploying at least some additional monitors not only improves fault-localization accuracy, but it also significantly improves explainability of the ML model reasoning, increasing the sense of trust towards the model and fostering adoption of these ML tools for fault management. In future work we will investigate if this conclusion remains true for practical deployments, by analyzing ML reasoning in larger mesh networks.

Acknowledgement. This work was partly supported by National Science Foundation (NSF), Japan-US Network Opportunity 2 (JUNO2), Grant No. 1818972.

REFERENCES

- [1] F. Musumeci et.al., “A Tutorial on Machine Learning for Failure Management in Optical Networks,” in IEEE/OSA Journal of Lightwave Technology, vol. 37, no. 16, pp. 4125-4139, Aug. 2019.
- [2] F. Musumeci et.al., “Domain Adaptation and Transfer Learning for Failure Detection and Failure-Cause Identification in Optical Networks Across Different Lightpath,” in IEEE/OSA Journal of Optical Communications and Networking, vol. 14, n. 2, pp. A91-A100, Feb. 2022.
- [3] L. Velasco and D. Rafique, “Fault Management Based on Machine Learning [Invited],” in Optical Fiber Communication Conference 2019, OSA Technical Digest (Optica Publishing Group, 2019), paper W3G.3.
- [4] K. S. Mayer et.al., “Soft Failure Localization Using Machine Learning with SDN-based Network-wide Telemetry,” at 2020 European Conference on Optical Communications (ECOC), pp. 1-4, Dec. 2020.
- [5] Deutsche Telekom, Guidelines for Artificial Intelligence whitepaper: <https://www.telekom.com/resource/blob/630952/37534d39c5184b251c235d93edfd6f91/dl-210702-professionsethik-data.pdf>
- [6] 5GPP, AI and ML – Enablers for Beyond 5G Networks report: <https://5g-ppp.eu/wp-content/uploads/2021/05/AI-MLforNetworks-v1-0.pdf>
- [7] S. M. Lundberg, L. Su-In Lee, “A Unified Approach to Interpreting Model Predictions,” Proceedings of the 31st International Conference on Neural Information Processing Systems, 2017.